

Interferometric microseism localization for multistage fracture monitoring

Oleg V. Poliannikov and Alison Malcolm, Earth Resources Laboratory, MIT, Cambridge, MA

Hugues Djikpesse and Michael Prange, Schlumberger-Doll Research, Cambridge, MA

Copyright 2011, SBGf - Sociedade Brasileira de Geofísica.

This paper was prepared for presentation at the Twelfth International Congress of the Brazilian Geophysical Society, held in Rio de Janeiro, Brazil, August 15-18, 2011.

Contents of this paper were reviewed by the Technical Committee of the Twelfth International Congress of The Brazilian Geophysical Society and do not necessarily represent any position of the SBGf, its officers or members. Electronic reproduction or storage of any part of this paper for commercial purposes without the written consent of The Brazilian Geophysical Society is prohibited.

Abstract

We show how interferometric methods can be used to improve the location of microseismic events when those events come from several different fractures and are observed from a single well. This is the standard setup for a multi-stage hydraulic fracturing experiment. Traditionally, in such experiments each event is located separately. Here, we adapt the interferometric approach to the problem of locating events relative to one another and show that this reduces the uncertainty in location estimates. To completely recover the Green's function between two events with interferometry requires a 2D array of receivers. When only a single observation well is available, we do not attempt to recover the full Green's function, but instead perform a partial redatuming of the data allowing us to reduce the uncertainty in two of the three components of the event location.

Introduction

Hydraulic fracturing is the process of injecting high-pressure fluids into a reservoir to induce fractures and thus improve reservoir productivity. Microseismic event localization is used to locate the created fractures. Traditionally, events are localized individually. Available information about events already localized is not used to help estimate other source locations (Huang et al., 2006; Bennett et al., 2006; Michaud et al., 2004). However, in applications where multiple fractures are created, previously located events in a reference fracture may provide redundant information about unknown events in subsequent fractures, improving estimates of the event positions. We propose to use events in fractures closer to the monitoring well, which should be better localized, to help locate events in farther fractures. It is known through seismic interferometry that with a 2D array of receivers, the travel time between two sources may be recovered from a cross-correlogram of two common source gathers (Wapenaar et al., 2005; Curtis et al., 2009). This allows an event in the second fracture to be localized relative to an event in the reference fracture. However, when the receiver array is 1D, classical interferometry cannot be directly employed because the problem becomes underdetermined. In our approach, interferometry is used to partially redatum microseismic events from a second

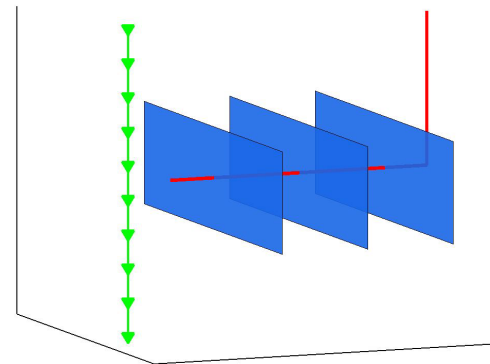


Figure 1: Water is injected under pressure through the treatment well (red curve), which creates multiple fractures (blue planes). The process is seismically monitored from the observation well (green). These fractures are shown as planes, but in practice are complex shapes that are localized as clouds of points.

fracture onto the reference fracture so that they can be used as virtual receivers, providing additional information complementary to that provided by the physical receivers, and thus resulting in more accurate location estimates as compared to traditional methods.

Problem setup

Assume that we have an estimate of the velocity model. Assume also that we have a monitoring well instrumented with three-component receivers with locations denoted \mathbf{x}_{rec} . The signals recorded at the receivers are seismograms that are assumed to contain direct arrivals from each event in each of two fractures. We also assume that the observed seismograms are perturbed by additive uncorrelated Gaussian noise that models measurement errors. Denote the two fractures as \mathcal{F}_1 and \mathcal{F}_2 , and assume that \mathcal{F}_1 is closer to the monitoring well than \mathcal{F}_2 . Although the two fractures are depicted in Figure 1 as being parallel to one another, this is not a necessary assumption. Indeed, the events on a fracture are localized independently of each other, and thus *no* geometry is imposed on the shape of the fracture. We also assume for simplicity that the events of the reference fracture, \mathcal{F}_1 , have been located precisely, although the method can handle uncertainty in reference event locations (Poliannikov et al., 2011).

Interferometric event localization

Classical localization

We use a simplified version of a classical localization technique as a point of comparison for our proposed interferometric method. We pick the travel time, t_p , of the P-wave from the event to the receiver using a cross-correlation method with a known source wavelet. Then we estimate the unit polarization vector, \hat{p} , of the P-wave using a method based on a singular value decomposition analysis of the arrival of the P-wave (de Franco and Musacchio, 2001). The polarization is a unit-length vector pointing from the receiver location \mathbf{x}_{rec} in the direction from which the wave impinges on the receiver. The source location is found by tracing a ray that leaves the receiver in the \hat{p} direction and stops at time t_p . This localization method is perfect if the medium is known exactly and the observed signal contains no noise. Random noise in the seismograms results in localization uncertainty, which can be reduced by stacking over multiple receivers.

Classical interferometry

Seismic interferometry allows physical sources to be redatumed to receiver locations (Rickett and Claerbout, 1996; Derode et al., 2003; Schuster et al., 2004; Bakulin and Calvert, 2004; Wapenaar et al., 2005; Djikpesse et al., 2009). Receivers can likewise be redatumed to source locations according to the principle of reciprocity (Curtis et al., 2009).

The cross-correlation lag of two direct arrivals from two different sources is a function, $\tau(\mathbf{x}_{\text{rec}})$, of the receiver position, \mathbf{x}_{rec} , that belongs to the 2D surface \mathcal{W} . The stationary phase point ($\mathbf{x}_{\text{rec}}^0, \tau(\mathbf{x}_{\text{rec}}^0)$) is defined by the extremum of the function τ . The stationary receiver location, $\mathbf{x}_{\text{rec}}^0$, marks the receiver that records the ray connecting the two sources. The stationary value, $\tau(\mathbf{x}_{\text{rec}}^0)$, has the physical meaning of the travel time between the two sources along that ray.

In classical interferometry, receivers enclosing the two sources must span a 2D surface \mathcal{W} . The stationary phase point is found by setting the two partial derivatives of τ in orthogonal directions to zero. Since only one partial derivative can be estimated with a 1D receiver array, the stationary phase condition becomes underdetermined (Figure 2(a)). Stationary points along a 1D receiver array, i.e., in a single monitoring well, are thus not stationary in the classical sense, but they still give useful information for source localization.

Interferometry using a single monitoring well

Although our method is valid for any (known) velocity model as well as for deviated wells, for clarity we consider here the case of a layered velocity model and a vertical monitoring well. In this case, interferometry allows us to use known events, $\mathbf{x}_{s,1}$, in a reference fracture \mathcal{F}_1 , to constrain two out of the three location parameters of an unknown microseism, $\mathbf{x}_{s,2}$ in \mathcal{F}_2 , and these parameters have a very clear intuitive meaning.

We first note that the azimuth of any event cannot be recovered from kinematics because the travel time in a layered medium from any source location to the vertical monitoring well does not depend on the azimuth of the

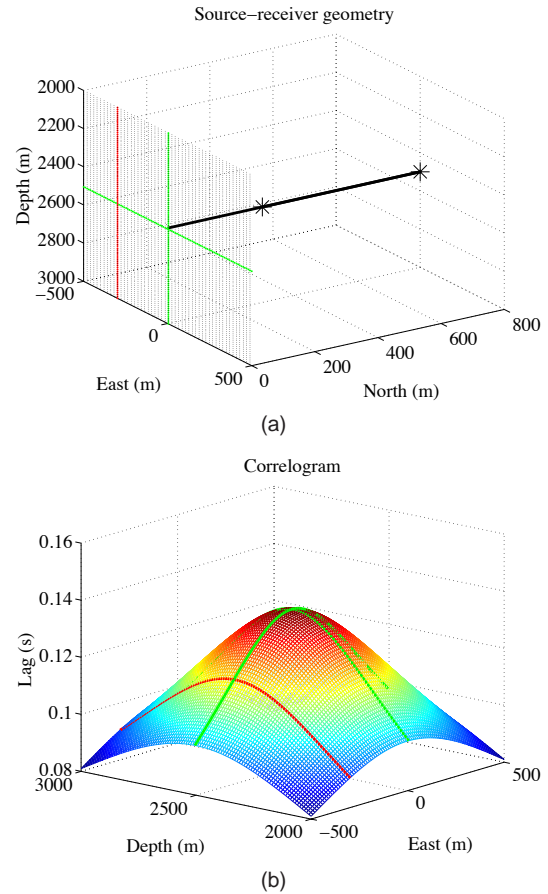


Figure 2: (a) The ray that connects two sources is received at a stationary receiver location within a two-dimensional receiver-array aperture (the intersection of the two green lines). (b) The stationary receiver location is the stationary point of the 2D correlogram. The stationary point is shown as the intersection of two common source gather lags plotted as green curves. A correlogram calculated over a one dimensional receiver array (red line) may exhibit an extremum, but it need not correspond to any physical ray or yield a physical travel time.

source. We can, however, recover the remaining spatial parameters of the event.

Indeed, consider two event locations, $\mathbf{x}_{s,1}$ and $\mathbf{x}_{s,2}$, where $\mathbf{x}_{s,1}$ is a known event from the reference fracture \mathcal{F}_1 and $\mathbf{x}_{s,2}$ is unknown event from the second fracture \mathcal{F}_2 that we will attempt to localize. The cross-correlogram of the two common event gathers contains an event from the correlations of the two direct waves with the lag, which is a function $\tau(z_{\text{rec}})$. The receiver located at $\mathbf{x}_{\text{rec}}^0$ is stationary in the z -direction for the pair of events $\mathbf{x}_{s,1}$ and $\mathbf{x}_{s,2}$, i.e. $\tau'(z_{\text{rec}}^0) = 0$, if they can be rotated around the axis of the monitoring well so as to lie on the same ray that begins from $\mathbf{x}_{\text{rec}}^0$ as shown in Figure 3. The stationary lag, $\tau(z_{\text{rec}}^0)$, is the physical travel time between the two rotated sources along this ray.

Each event location $\mathbf{x}_{s,2}$ can be defined with three spatial parameters: the take-off angle, θ_2 , of the ray that connects the stationary receiver $\mathbf{x}_{\text{rec}}^0$ and $\mathbf{x}_{s,2}$, the travel

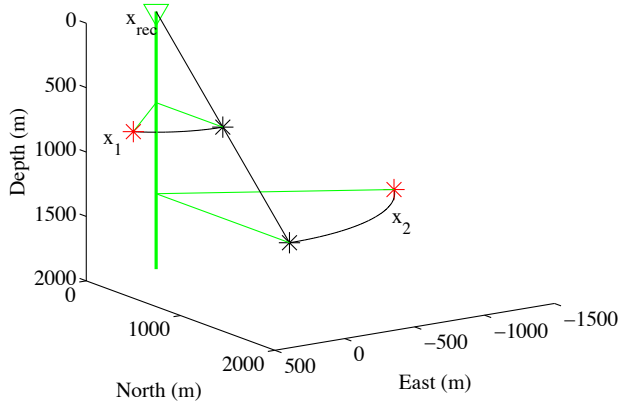


Figure 3: The receiver in a 1D array is vertically stationary with respect to two given sources (red stars) if the source locations can be rotated about the receiver line into collinear positions (black stars).

time, $T(\mathbf{x}_{\text{rec}}^0, \mathbf{x}_{s,2})$, from the stationary receiver to the event location along the ray, and the azimuthal angle. Knowing the location of a reference event $\mathbf{x}_{s,1}$, we can recover the first two spatial parameters of the location $\mathbf{x}_{s,2}$ of the unknown event:

$$\begin{aligned} \theta_2 &= \theta_1, \\ T(\mathbf{x}_{\text{rec}}^0, \mathbf{x}_{s,2}) &= T(\mathbf{x}_{\text{rec}}^0, \mathbf{x}_{s,1}) + \tau(\mathbf{x}_{\text{rec}}^0). \end{aligned} \quad (1)$$

Instead of the take-off angle and the travel time, we can equivalently recover the horizontal offset and the depth of the event location.

Figure 4 illustrates how event localization using a neighboring fracture works when the known fracture is planar. Any event $\mathbf{x}_{s,1}$ lying at the intersection of fracture \mathcal{F}_1 with the surface defined by a constant take-off angle from the fixed receiver $\mathbf{x}_{\text{rec}}^0$ will produce a stationary point at the same stationary receiver depth z_{rec}^0 . The stationary lags, $\tau(z_{\text{rec}}^0)$, will vary depending on $\mathbf{x}_{s,1}$. However, the travel time from the receiver to the unknown location can always be computed from the location of any reference source and the stationary lag using Equation 1. Because the total number of sources in fracture \mathcal{F}_1 is typically large, we can expect to have many redundant measurements of the take-off angle and radial distance of $\mathbf{x}_{s,2}$. We can use these to boost the signal-to-noise ratio to obtain more precise estimates by appropriate averaging.

Numerical example

In this section, we illustrate the performance of the proposed algorithm with a synthetic experiment. We compare the accuracy of the localization by the classical localization algorithm to the improved interferometric one.

The monitoring well is placed vertically at $(x_{\text{rec}}, y_{\text{rec}}) = (0, 0)$ m. 20 three-component receivers are placed in the well equidistantly at depths from 2150 to 2450 m (Figure 5a). The model consists of three layers with interfaces at depths 2200 and 2380 m (Figure 5b). The respective velocities are 3500, 3600 and 3700 m/s. Two vertical planar fractures are positioned next to a monitoring well at a depth of 2300 m. The reference fracture is positioned 100 m away from the

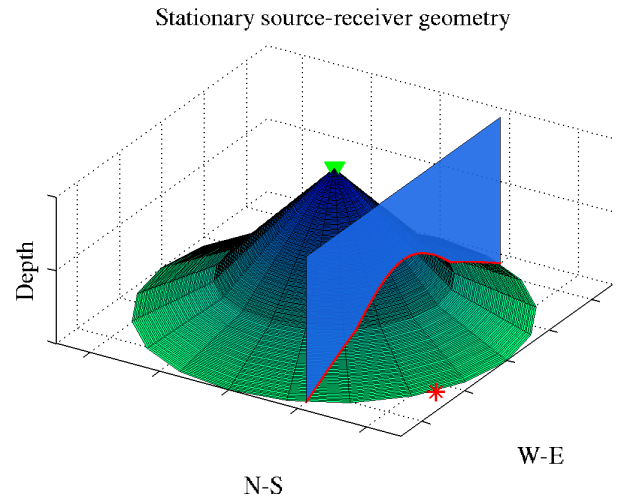


Figure 4: For a layered medium, the unknown take-off angle (or horizontal offset) and distance along the ray of a source (red star) can be estimated with the help of many stationary sources in the neighboring fracture (vertical plane). Any source along the red curve provides an independent measurement of the distance and horizontal offset of an unknown microseism.

well, and the second fracture is 200 m away. Both fractures are 300 meters wide and 100 meters tall. Microseisms are simulated by placing 625 sources on a rectangular grid inside the reference fracture (25 in each direction). All source locations in the first fracture are assumed to be known exactly.

For illustration purposes, we put just a single source in the second fracture at $\mathbf{x}_{s,2} = (200, 0, 2300)$ m. The source is a Ricker wavelet (the first derivative of a Gaussian) with a central frequency of 50 Hz. The seismograms are computed using the discrete wavenumber method (Bouchon, 1981) and the reflectivity method (Müller, 1985), and are then contaminated with additive, uncorrelated, Gaussian noise. The signal-to-noise ratio, defined as the ratio of the peak amplitude to the standard deviation of the noise, is approximately 3 in our experiment.

Localization of the event at $\mathbf{x}_{s,2}$ is attempted based on the noisy seismogram using the classical and the proposed method. The workflow is as follows. We generate 200 independent realizations of noisy seismograms. For each noisy realization, we localize the source using the classical approach and plot it as a blue dot in Figure 6. Because the proposed method is unable to improve the estimate of the azimuth, we present results in the horizontal offset-depth domain.

The blue dots form a cloud centered around the true location of the source. The standard deviation of the error in estimated offset of the standard method in this case is approximately 4.5 m. The standard deviation of the depth error is approximately 3.36 m.

We locate the same source with the same geometry using the interferometric method presented here and the microseism locations in the reference fracture. According to the theory, for all events $\mathbf{x}_{s,1}$ in the reference fracture

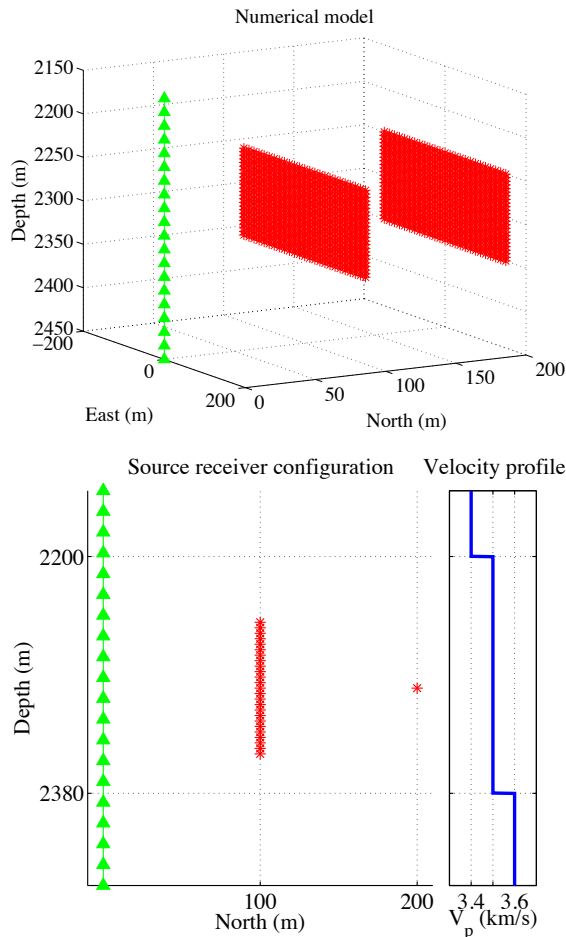


Figure 5: The numerical model contains a monitoring well with two vertical fractures nearby. A source in the more distant fracture is localized using 625 microseismic sources in the nearer fracture.

we correlate their seismograms with those of the unknown microseism, and we find the stationary condition of the event in the correlogram, which consists of a stationary receiver and a stationary lag.

A ray is traced from the stationary receiver through the event $x_{s,1}$, and the location $x_{s,2}$ is measured on it using the stationary lag as the travel time between the two points. The location of $x_{s,2}$ can be estimated in a layered medium only up to an unknown azimuth. However, both the horizontal offset and the depth are recovered. We show the offset and depth of $x_{s,2}$ so obtained as green stars in Figure 6.

Plotting the interferometric estimates shows a big improvement over the traditional method. The cloud is distributed much closer the true location. The standard deviation of the error in estimated offset of the interferometric method is 0.52 m, and the standard deviation of the depth error is 0.94 m. Therefore, the improvement in localizing the source is about a factor of 3.6 in depth and 9 in offset. While specific results of this experiment may not translate to other experimental configurations, the superior performance of the interferometric method in this configuration is evident.

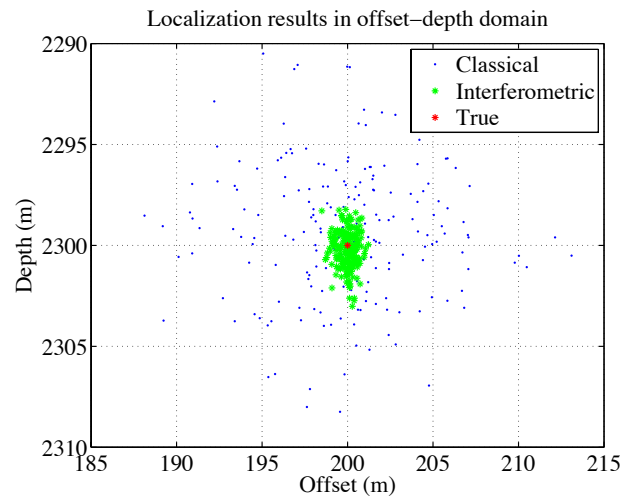


Figure 6: Localization results plotted in the offset-depth domain. The new method offers significantly improved estimates.

Conclusions

Microseism event localization remains an important and challenging problem. Classical algorithms tend to locate events individually without fully exploiting the coupling and redundancy that exists in the recorded data for multiple fractures. We have considered a problem with two fractures and a single monitoring well. This prototype is typical in hydrofracture monitoring applications where multiple fractures are sequentially created to improve fluid production. When some fractures are known better than others, we propose to use interferometry to image the less well-located fractures relative to those with more accurate locations. We demonstrate the effectiveness of our methodology on a layered model with a vertical well, although the method can be generalized to an arbitrary velocity model. Applying classical interferometry in a 3D medium requires a 2D array of receivers. When the available data is one-dimensional, basic concepts such as the stationary phase point are not uniquely defined, and consequently standard techniques are not applicable. For a vertical array of receivers, the azimuth information is lost. We have shown that estimates of both horizontal offset and depth can be significantly improved using interferometric techniques.

Acknowledgements

The authors would like to thank the ERL Founding Members Consortium, Schlumberger-Doll Research and particularly Stéphane Rondenay for their support of this work.

References

- Bakulin, A., and R. Calvert, 2004, Virtual source: new method for imaging and 4D below complex overburden: Expanded Abstracts, SEG's 74th Annual Meeting, 2477–2480.
- Bennett, L., J. L. Calvez, D. R. R. Sarver, K. Tanner, W. S. Birk, G. Waters, J. Drew, G. Michaud, P. Primiero, L. Eisner, R. Jones, D. Leslie, M. J. Williams, J. Govenlock, R. C. R. Klem, and K. Tezuka, 2005–2006, The source

- for hydraulic fracture characterization: *Oilfield Review*, **17**, 42–57.
- Bouchon, M., 1981, A simple method to calculate Green's functions for elastic layered media: *Bulletin of the Seismological Society of America*, **71**, 959–971.
- Curtis, A., H. Nicolson, D. Halliday, J. Trampert, and B. Baptie, 2009, Virtual seismometers in the subsurface of the Earth from seismic interferometry: *Nature Geoscience*, **2**, 700–704.
- de Franco, R., and G. Musacchio, 2001, Polarization filter with singular value decomposition: *Geophysics*, **66**, 932–938.
- Derode, A., E. Larose, M. Campillo, and M. Fink, 2003, How to estimate the Green's function of a heterogeneous medium between two passive sensors? Application to acoustic waves: *Applied Physics Letters*, **83**, 3054–3056.
- Djikpesse, H., S. Dong, J. Haldorsen, and D. Miller, 2009, Comparing interferometric migration and mirror imaging of 3D VSP free-surface multiples: *Noise and Diffuse Wavefields: DGG-Mitteilungen*, German Geophysical Society, 79–86.
- Huang, Y. A., J. Chen, and J. Benesty, 2006, Time delay estimation and acoustic source localization, *in* *Acoustic MIMO Signal Processing: Springer US, Signals and Communication Technology*, 215–259.
- Michaud, G., D. Leslie, J. Drew, T. Endo, and K. Tezuka, 2004, Microseismic event localization and characterization in a limited aperture HFM experiment: *SEG Expanded Abstracts*, **23**.
- Müller, G., 1985, The reflectivity method: a tutorial: *Journal of Geophysics*, **58**, 153–174.
- Poliannikov, O. V., A. Malcolm, H. Djikpesse, and M. Prange, 2011, Interferometric hydrofracture microseism localization using neighboring fracture: *Geophysics*, *in press*.
- Rickett, J., and J. Claerbout, 1996, Passive seismic imaging applied to synthetic data: Technical Report 92, Stanford Exploration Project. (<http://sepwww.stanford.edu/public/docs/sep92/james1.ps.gz>).
- Schuster, G. T., J. Yu, J. Sheng, and J. Rickett, 2004, Interferometric/daylight seismic imaging: *Geophysical Journal International*, **157**, 838–852.
- Wapenaar, K., J. T. Fokkema, and R. Snieder, 2005, Retrieving the Green's function in an open system by cross correlation: a comparison of approaches: *Journal of the Acoustical Society of America*, **118**, 2783–2786.